Journal of the Nigerian Association of Mathematical Physics
Volume 10 (November 2006), **47 - 58**

A 2-dimensional finite element simulation of cooling in castings

John A. Akpobi and Imafidon A. Lawani.
Department of Production Engineering, University of Benin, Nigeria

Abstract

In this work we present a 2 dimensional finite element simulation of the cooling process in castings. A one way coupling +technique was used to predict the behavior of thermal strains and stresses from the temperature history of casting. The temperature distribution across the casting at different times, the cooling pattern of the casting in different cooling media, the cooling times and the build up of thermal strains and stresses were simulated in this work. The model was validated with experimental cooling times in the scenarios considered.

Keywords: Casting, one way coupling, thermal history, thermal strains and stresses.

1.0 Introduction

The nature of cooling in a casting determines the quality of the casting obtained [1]. This could be affected by several factors such as the cooling media and type of mould. In designing a part to be cast, the use of experimental methods to study the characteristics of the final product is in no doubt expensive. The use of numerical simulations during the design stage of a product is becoming increasingly popular. This is due to the fact that the cost very little and are more accurate.

In this work, we explore the use of the finite element method in the study of cooling vis a vis the casting process. The temperature history of the castings is first obtained from a finite element based model. A one way coupling technique was then used to interface this model with a strain/stress model in order to study the behavior of thermal strains and stresses.

2. Finite element modelling

The modeling technique adopted is based on a one way coupling technique which has been effectively used in welding simulations [5]. . The temperature history is first obtained from a finite element model based on the heat conduction equation. The temperature history is then fed in to plane stress based finite element model in form of thermal gradients converted to thermal strains.

Notation

C	Heat capacity.
E	Young's modulus.
E_c	Constitutive matrix.
F	Flux vector.
$f_{x,y}$	Body forces.
h	Convective heat transfer coefficient, height of element.
K	Stiffness Matrix.
k	Coefficient of heat conduction.
M	Mass Matrix.
n	Number of nodes
$n_{x,y}$	The components (or direction cosines) of the unit normal vector $\hat{n}$.
$\hat{n}$	Unit normal vector on the boundary, Γ.
Q	Flux.
T	Temperature.

.

$\dot{T}$	Temperature derivative.
T_{ext}	External Temperature.
T_j	The value of $T(x, y, t)$ at the spatial location (x_j, y_j) at time t.
t	Time.
ΔT	Change in Temperature.
Δt	Time step.
u, v	Displacements in x and y directions.
α	Coefficient of linear expansivity
ε	Normal strain.
$\varepsilon_{x,y}$	Normal strains in indicated direction.
γ_{xy}	Shear strain.
ν	Poisson's ratio.
ρ	Density.
σ	Normal stress.
$\sigma_{x,y}$	Normal strains in indicated direction.
τ_{xy}	Shear stress.
$\hat{t}_{x,y}$	Specified boundary stresses.
∇	Laplacian operator.
Γ	Boundary.
Ω	Domain.
Ψ_i	Interpolation functions.

The reason for this one way coupling, is based on the fact that changes in the temperature of the casting affect the strains and stresses in the casting but the changes in the strains and stresses do not affect the temperature of the system.

Cooling in the casting process is based on the heat conduction equation taking into consideration boundaries subject to convection. The general equation used to describe this is given as ([4] and [2]):

$$\rho c\frac{\partial T}{\partial t}-\nabla(k\nabla T)=h(T_{ext}-T) \qquad (2.1)$$

subject to the initial condition: $\{T\}_0=\{T_0\}$.

The finite element model developed to simulate cooling in the casting process is based on equations (2.1) and (2.2). In selecting an approximation for temperature, T, it is assumed that time can be separated from the spatial variation ([3] and [2]), that is: $T(x,y,t)\approx\sum_{j=1}^{n}T^{e}{}_{j}(t)\psi^{e}{}_{j}(x,y)$ (2.2)

Equation (2.2) constitutes the nature of the solution to be computed at each time step. The finite element model obtained, based on this, is: $0=\sum_{j=1}^{n}\left(M^{e}{}_{ij}\frac{dT^{e}{}_{j}}{dt}+K^{e}{}_{ij}T^{e}{}_{ij}\right)-F^{e}{}_{i}$ (2.3)

or in matrix form, $[M^e]\{\dot{T}^e\}+[K^e]\{T^e\}=\{F^e\}$ (2.4)

where a superposed dot on T denotes the time derivative, and $M^{e}_{ij}=\int_{\Omega^e}\rho c\Psi_i\Psi_j dxdy$, $K^{e}_{ij}=\int_{\Omega^e}k\left(\frac{\partial\Psi_i}{\partial x}\frac{\partial\Psi_j}{\partial x}+\frac{\partial\Psi_i}{\partial y}\frac{\partial\Psi_j}{\partial y}\right)dxdy$

$$F^{e}=\int_{\Omega^e}h(T_{ext}-T)\Psi_i dxdy \qquad (2.5)$$

This completes the *semidiscrete* finite element model (for cooling) over an element.

The model developed to study the thermal strains and stresses, (assuming isotropic conditions) is based on [2].

$$\begin{Bmatrix}\sigma_x\\ \sigma_y\\ \tau_{xy}\end{Bmatrix}=\frac{E}{1-\nu^2}\begin{bmatrix}1 & \nu & 0\\ \nu & 1 & 0\\ 0 & 0 & (1-\nu)/2\end{bmatrix}\begin{Bmatrix}\varepsilon_x\\ \varepsilon_y\\ \gamma_{xy}\end{Bmatrix} \qquad (2.6)$$

The deformation of the material is described by displacements in the x and y directions, u and v, from which the strains are defined as: $\varepsilon_x=\frac{\partial u}{\partial x},\varepsilon_y=\frac{\partial v}{\partial y},\gamma_{xy}=\frac{\partial u}{\partial y}+\frac{\partial v}{\partial x}$ (2.7)

The balance of force equations are:

$$-\frac{\partial \sigma_x}{\partial x}-\frac{\partial \tau_{xy}}{\partial y}=f_x$$
$$-\frac{\partial \tau_{xy}}{\partial x}-\frac{\partial \sigma_y}{\partial y}=f_x \qquad (2.8)$$

With boundary conditions:

$$\left.\begin{aligned} t_x &\equiv \sigma_x n_x+\sigma_{xy} n_y=\hat{t}_x \\ t_x &\equiv \sigma_{xy} n_x+\sigma_y n_y=\hat{t}_y \end{aligned}\right\} \qquad (2.9)$$

To express the above equations in elliptic form, substituting equation (2.6) into (2.8) results in:

$$-\frac{\partial}{\partial x}\left(c_{11}\frac{\partial u}{\partial x}+c_{12}\frac{\partial v}{\partial y}\right)-\frac{\partial}{\partial y}\left[c_{33}\left(\frac{\partial u}{\partial y}+\frac{\partial v}{\partial x}\right)\right]=f_x$$
$$-\frac{\partial}{\partial y}\left[c_{33}\left(\frac{\partial u}{\partial y}+\frac{\partial v}{\partial x}\right)\right]-\frac{\partial}{\partial y}\left(c_{12}\frac{\partial u}{\partial x}+c_{22}\frac{\partial v}{\partial y}\right)=f_y \qquad (2.10)$$

The boundary stress components (or tractions) can also be expressed in terms of the displacements:

$$t_x=\left(c_{11}\frac{\partial u}{\partial x}+c_{12}\frac{\partial v}{\partial y}\right)n_x+c_{33}\left(\frac{\partial u}{\partial y}+\frac{\partial v}{\partial x}\right)n_y$$
$$t_y=c_{33}\left(\frac{\partial u}{\partial y}+\frac{\partial v}{\partial x}\right)n_x+\left(c_{12}\frac{\partial u}{\partial x}+c_{22}\frac{\partial v}{\partial y}\right)n_y \qquad (2.11)$$

where $$c_{11}=c_{22}=\frac{E}{1-v^2},\ c_{12}=c_{21}=vc_{11}=vc_{22},\ c_{33}=\frac{E}{2(1+v)} \qquad (2.12)$$

u and *v* are approximated over an element by: $$u\approx\sum_{j=1}^{n}u_j^e\psi_j^e(x,y),\ v\approx\sum_{j=1}^{n}v_j^e\psi_j^e(x,y) \qquad (2.13)$$

The finite element model for stress is then obtained as:

$$\begin{bmatrix}[K^{11}] & [K^{12}]\\ [K^{12}]^T & [K^{22}]\end{bmatrix}\begin{Bmatrix}\{u\}\\ \{v\}\end{Bmatrix}=\begin{Bmatrix}\{F^1\}\\ \{F^2\}\end{Bmatrix} \qquad (2.14)$$

where

$$K_{ij}^{11}=\int_{\Omega^e}h\left(c_{11}\frac{\partial\psi_i}{\partial x}\frac{\partial\psi_j}{\partial x}+c_{33}\frac{\partial\psi_i}{\partial y}\frac{\partial\psi_j}{\partial y}\right)dxdy\ K_{ij}^{12}=K_{ji}^{21}=\int_{\Omega^e}h\left(c_{12}\frac{\partial\psi_i}{\partial x}\frac{\partial\psi_j}{\partial y}+c_{33}\frac{\partial\psi_i}{\partial y}\frac{\partial\psi_j}{\partial x}\right)dxdy$$
$$K_{ij}^{22}=\int_{\Omega^e}h\left(c_{33}\frac{\partial\psi_i}{\partial x}\frac{\partial\psi_j}{\partial x}+c_{22}\frac{\partial\psi_i}{\partial y}\frac{\partial\psi_j}{\partial y}\right),\ F_i^1=\int_{\Omega^e}h\psi_i f_x dxdy+\int_{\Gamma^e}h\psi_i t_x ds,\quad F_i^1=\int_{\Omega^e}h\psi_i f_y dxdy+\int_{\Gamma^e}h\psi_i t_y ds \qquad (2.15)$$

3.0 Implementation

The models presented above were then carefully solved to obtain numerical and graphical visualizations using MATLAB software. The implementation was in two phases. The first phase was to simulate the cooling process and thus obtain the temperature history of the casting. The thermal history was then fed into the strain/stress model as thermal strains based on the temperature gradients existing in the casting during cooling.

Interfacing the cooling and stress models required some conversions. The nodal temperatures obtained from the cooling model are interpolated to obtain temperatures at the center of the triangular elements (see Figure 1). The reason for this is that the body forces in the stress model are assigned to each triangle and not nodes. The thermal strains are obtained from:

$$\varepsilon = \alpha\Delta T \qquad (3.1)$$

But these strains cannot be fed directly into the strain/stress model. They are converted to body forces with:

$$f_{x,y}=E_c\varepsilon \qquad (3.2)$$

An obvious advantage in the technique outlined above was the use of the same geometry and mesh for both models, thus avoiding errors that could have accrued as a result of model/mesh transformations.Table 1 shows the material properties used in the simulation

Material	Density (kg/m^3)	Heat Capacity (J/kg)	Coefficient of Heat Conduction (*W/m/K*)	Linear Expansivity (/K)	Modulus of Elasticity (GPa)	Poisson's Ratio
Cast Iron	7800.00	450.00	52.00	11×10^{-6}	198.00	0.27
Aluminium	2700.00	900.00	229.00	24×10^{-6}	70.00	0.33
Sand	78.00	0.19	0.95	1.2×10^{-6}	63.00s	0.29

4.0 Results

The technique outlined above was used in simulating the cooling of pure aluminum in various media. Figure 1 shows the discretized (104 nodes and 156 elements) geometry of the casting. The cooling times when the casting is cooled in water, air and sand mould was determined experimentally (see Table 2). Due to the objectives of the experiment and necessity of obtaining accurate data; immediately full solidification was observed, the casting was immediately freed from the mould and transferred into water (for the case of water cooling). And the cooling time monitored with the aid a digital temperature sensor, the time the cast took to cool down to water temperature, using a stop watch was taken and recorded. The experiments for cooling in air and sand mould were also monitored and their values recorded.

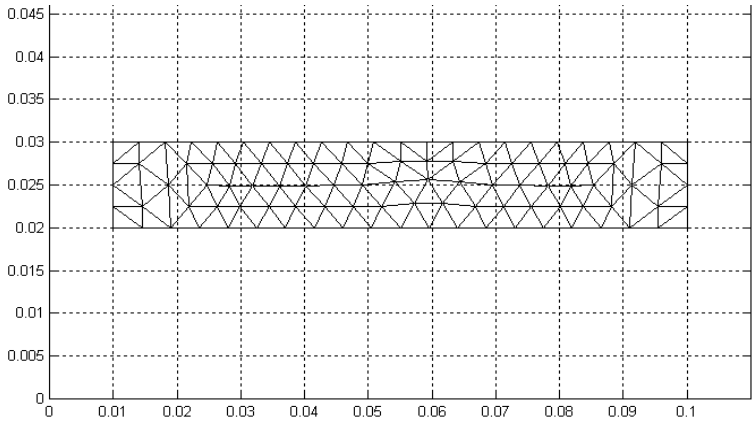

Figure 1: Discretized geometry of casting (units in meters)

The cooling times determined experimentally and from numerical simulation shown below in Table 2.

Table 2: Experimental and numerically simulated cooling times for various scenarios.

	Experiment	**Numerical Simulation**
Water Cooling	51.00 seconds	59.00 seconds
Air Cooling	50.00 minutes	53.33 minutes
Sand Mould Cooling	118.00 minutes	123.00 minutes

The temperature distribution at different times of the casting when cooled in water at different times is shown in Figure 2.

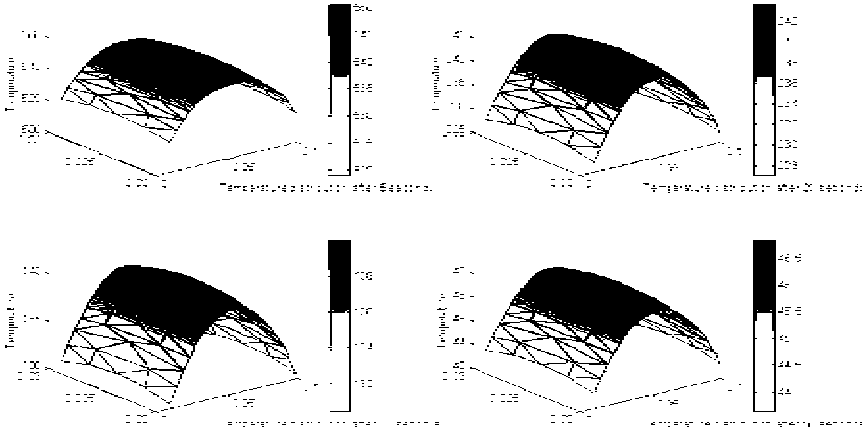

Figure 2: Temperature (^oC) distribution at different times (water-cooling of casting)

The cooling curve for the casting when cooled in water can be seen in Figure 3.

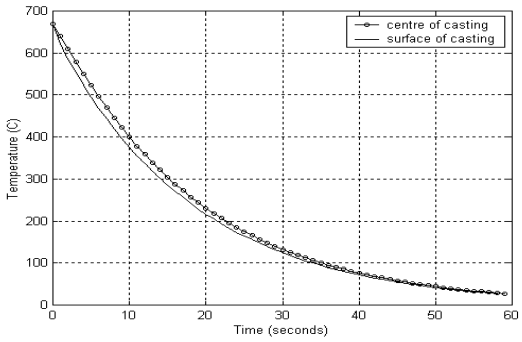

Figure 3: Cooling curve of casting (water-cooling)

The thermal strains and stresses as a result of the temperature gradients developed in the casting during cooling are considered next. The distribution of these strains and stresses of the casting when cooled in water is shown in Figure 4.

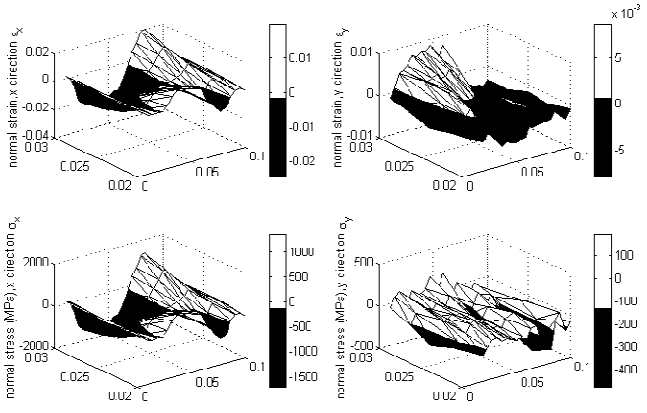

Figure 4: Distribution of thermal strains and stresses after cooling (water-cooling)

The build up of the strain and stresses on elements at the centre and surface of the casting is shown in Figure 5.

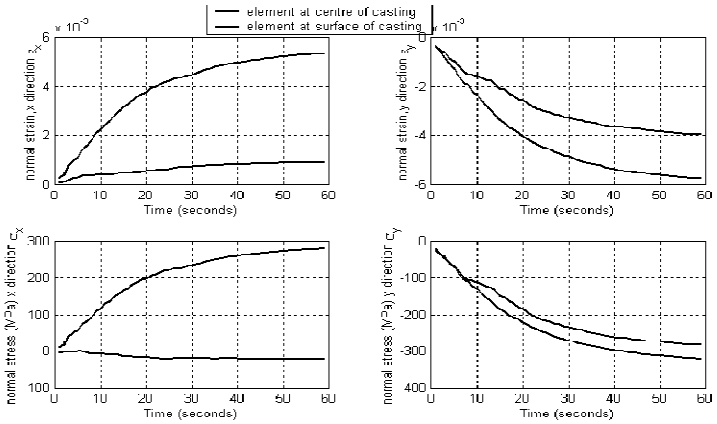

Figure 5: Build up of thermal strains and stress on elements at the surface and centre of casting (water-cooling)

Simulations of cooling the casting in air are considered next. The temperature distribution at different times is shown in Figure 6.

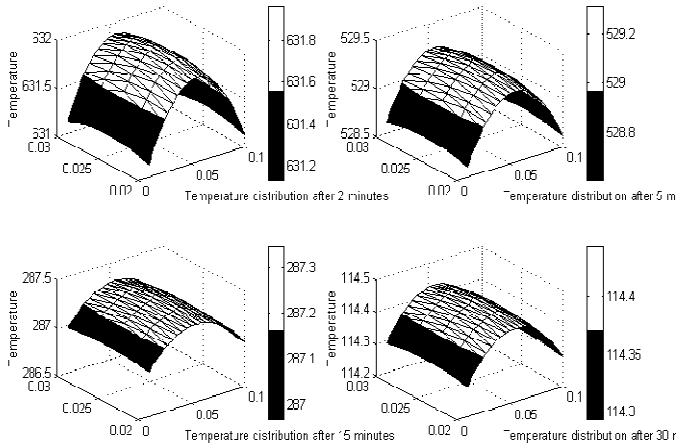

Figure 6: Temperature (ºC) distribution at different times (air-cooling of casting)

The cooling curve of the casting when cooled in air is also shown in Figure 7.

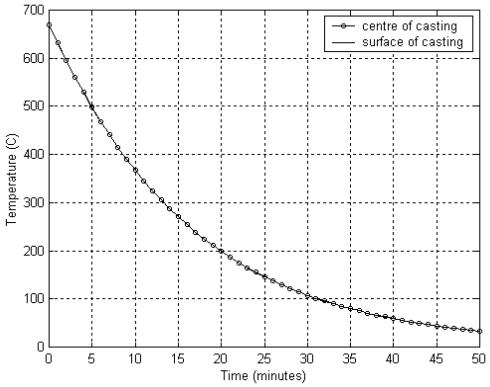

Figure 7: Cooling curve of casting (air-cooling)

The distribution of thermal strain and stresses when cooled in air to room temperature is shown in Figure 8.

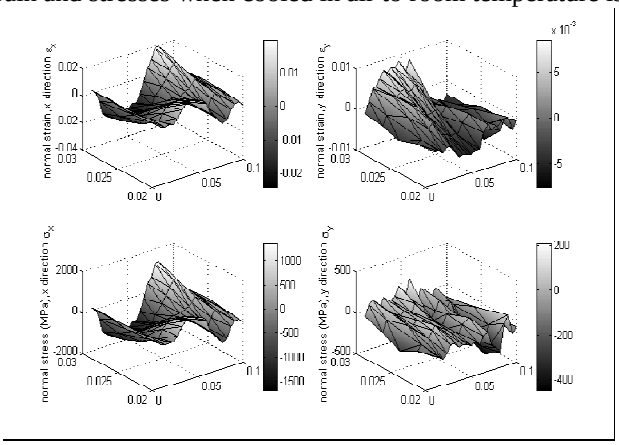

Figure 8: Distribution of thermal strains and stresses after cooling (air-cooling)

The build of these strains and stresses on elements at the centre and surface of the casting is shown in Figure 9.

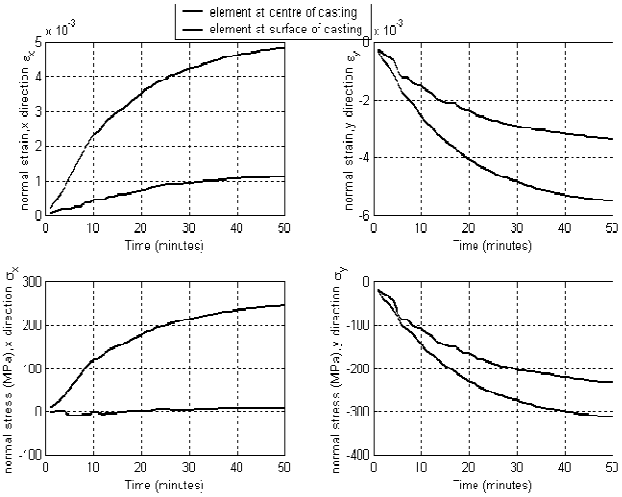

Figure 9: Build up of thermal strains and stress on elements at the surface and centre of casting (air-cooling)

Simulations of cooling in a sand mold with aluminum flask were considered next. The discretized (951 nodes and 1792 elements) geometry of the mold-casting arrangement is shown in Figure 10.

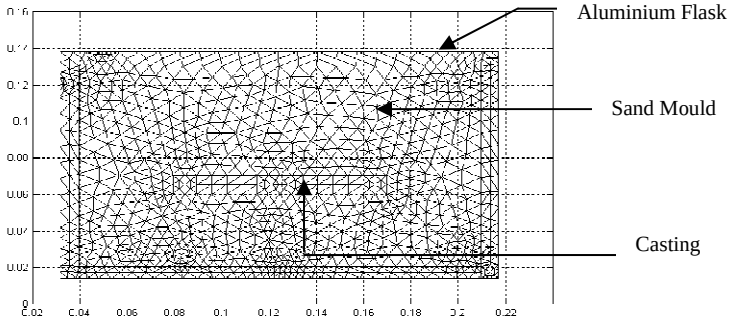

Figure 10: Discretized geometry (Aluminum flask-sand mold-casting arrangement), units in meters. The temperature distribution of the entire arrangement (with the mould originally at a room temperature of 32°C) at different times is shown in Figure 11.

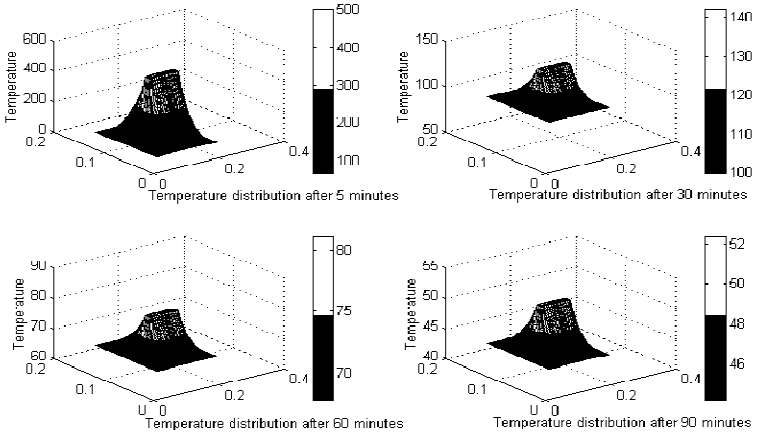

Figure 11: Temperature(°C) distribution at different times (sand mold-cooling of casting)

The cooling curve for the casting, elements near the mold-casting interface and elements at the surface of the aluminum flask is shown in Figure 12.

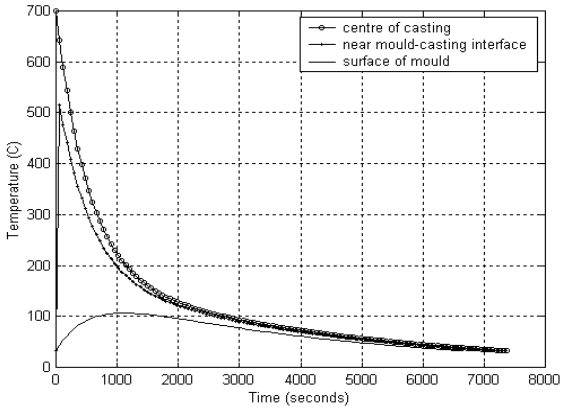

Figure 12: Cooling curve of casting (sand mold-cooling)

The distribution of thermal strains and stresses for the mold-casting arrangement is shown in Figure 13.

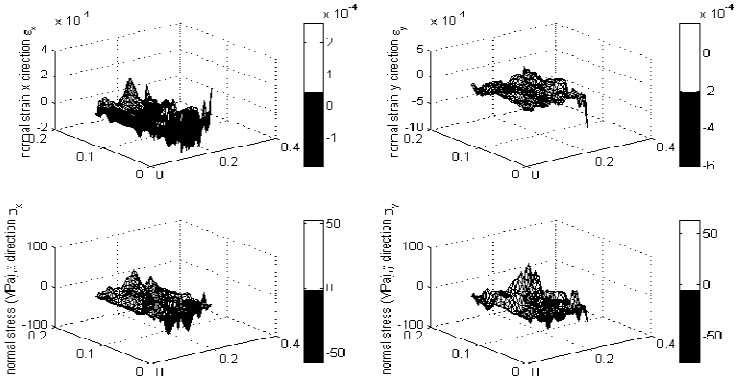

Figure 13: Distribution of thermal strains and stresses after cooling (sand mold-cooling)

The build up of these strains and stresses on elements at the centre and surface of the casting is shown in Figure 14.

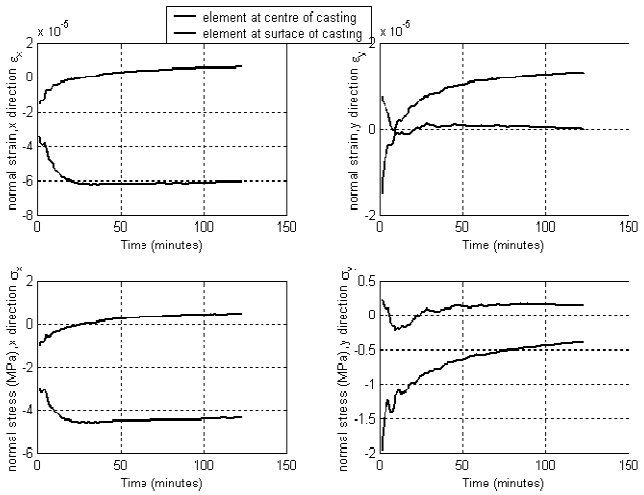

Figure 14: Build up of thermal strains and stress on elements at the surface and centre of casting (sand mold-cooling)

For a cast iron mould, similar simulations were carried out. The discretized (148 nodes and 260 elements) geometry is shown in Figure 15.

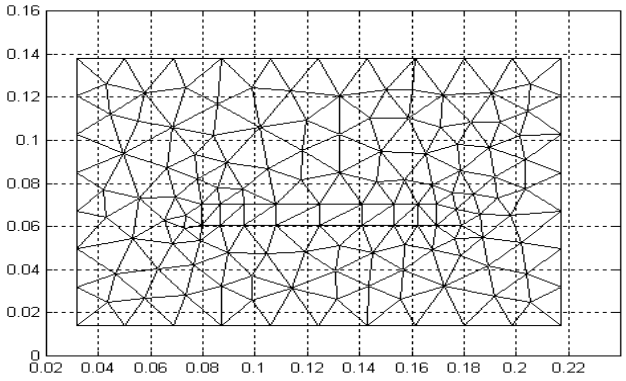

Figure 15: Discretized geometry (cast iron mold-casting arrangement)

The temperature distribution at different times is shown in Figure 16.

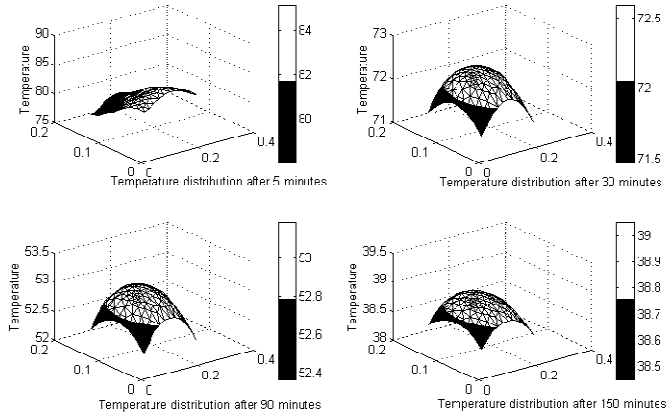

Figure 16: Temperature (°C) distribution at different times (cast iron mold-cooling of casting)

The cooling curve for several elements on the mold-casting arrangement is shown in Figure 17.

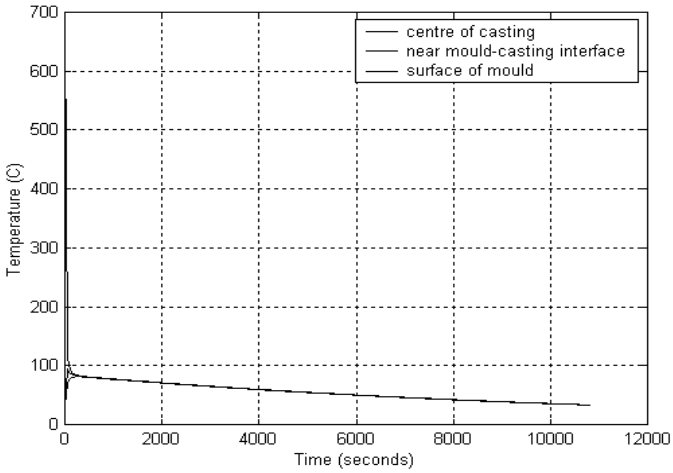

Figure 17: Cooling curve of casting (cast iron mold-cooling)

The thermal stains and stresses distribution is shown in Figure 18.

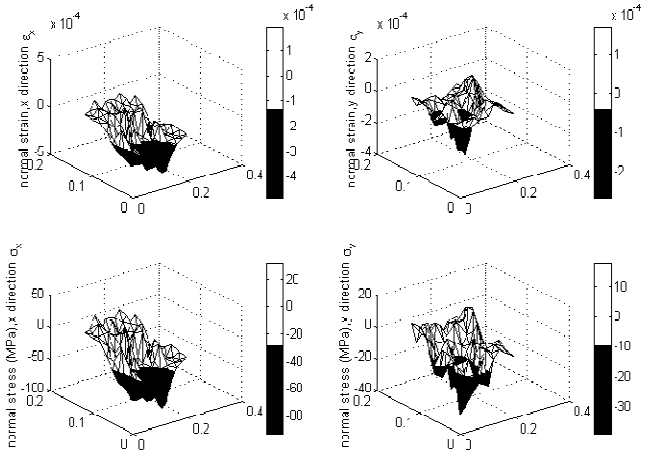

Figure 18: Distribution of thermal strains and stresses after cooling (cast iron mold-cooling)

The build up of thermal strains and stresses on elements at the centre and surface of the casting is shown in Figure 19.

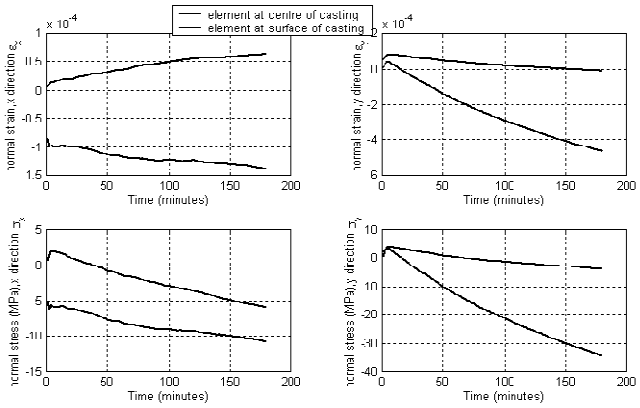

Figure 19: Build up of thermal strains and stress on elements at the surface and centre of casting (cast iron mold-cooling)

5. 0 Discussion

The results show that the simulated cooling times compare well with the values obtained from the experiments as can be seen from Tables 2. For cooling in water as can be seen from Figure 3, the cooling time is very fast (59 seconds) and the cooling pattern at the surface and centre of casting shows a relatively wider variance compared to cooling the casting in air (Figure 7), in which the variance is not obvious. The temperature distribution plots show the large temperature gradients in the casting. The overall temperature gradient after 5 seconds is about 20°C, which is quite high considering the size of the casting. This gradient drops to 2.5°C after 50 seconds. Even with the small size of casting, the surface and centre of the casting cool in a different pattern with a large variance as can be seen from the cooling curves. The plots for thermal strains normal to both *x* and *y* directions show that the maximum strain is about 0.03 (compressive and tensile) in the *x* direction. The strains in the *y* direction are of lower values. The compressive strains are complementary to the tensile strains, occurring in opposite directions to the tensile stresses. The normal stresses in *x* direction complement the results obtained from the thermal strains, with the highest tensile stresses above 1500 *MPa*. The highest compressive stresses are above 1000 *MPa* and are complementing the tensile stresses. Stresses normal to the *y* direction are evenly distributed with lesser variance than those obtained from stresses normal to the *x* direction. The maximum tensile and compressive stresses are above 400 *MPa* and 100 *MPa* respectively.

The temperature distribution of the casting when cooled in air is more even than when cooled in water. The highest temperature gradient in the casting as can be seen from Figure 6 above is about 0.6°C. In comparison with that developed for cooling in water, this is excellent. The congruent cooling pattern can be exemplified with the cooling curve. The thermal strains and stresses developed do not differ much from those developed from cooling in water. This is because the cooling patterns do not differ much but with only large differences in cooling times.

For cooling in a mould comprising aluminium flask and sand, nodes at the centre, mould-casting interface and the exterior of the mould were studied. For nodes at the centre of the casting (see Figure 12), the cooling curve shows a gradual decline in the temperature of the casting till it gets to room temperature. For nodes near the mould-casting interface, the cooling curve shows a sharp rise in the temperature before it begins to gradually decline. Nodes at the exterior of the mould show a gradual increase in temperature before it begins to drop. The temperature distribution around the casting does not show a variance of more than 2°C, which is also good. From the cooling curve (Figure 12), it can be seen that the sand heat up to about 400°C from room temperature just after pouring. But the aluminum flask just rises to a maximum of about 110°C before dropping steadily to room temperature. It will also be observed that the temperature of the cast drops rapidly in the first 15 minutes but slows down afterwards. In general, the molten metal heats up the system through conduction. Due to the thermal resistance of sand, the temperature rise at the aluminum flask is at a reduced rate compared to regions near the mould/molten metal interface. The effect of this on the cooling time can be seen in a large variance it takes for the aluminum flask, sand and the casting to achieve room temperature. The distribution of thermal strains and stresses is more controlled in this method of cooling as can be seen from Figure 13 with the strains varying from about 0.003(tensile) to about 0.0025(compressive) in *x* direction. These strains also reduce the thermal stresses markedly with stresses normal *x* direction with values from about 150 *MPa* (tensile) to 150 *MPa* (compressive) and those normal to the *y* having values ranging from 80 *MPa* (tensile) to 40 *MPa* (compressive).

The study was further extended to cooling, using a cast iron mould. The curves (Figure 17) show a faster drop in the temperature of the casting (due to its relatively high conduction coefficient when compared to sand) but overall, it takes a longer time to cool. This is not surprising, because cast iron has a very high heat capacity, and hence will not release its heat easily.

The simulation of the above experiment using a cast iron mould gives interesting perspective to the process. As expected, the temperature drop of the casting when compared with in sand mould was faster. From Figure 12**,** the maximum temperature of the casting in a sand mould, was about 500°C in 5 minutes, while from Figure 16, the maximum temperature in the casting was about 85°C in 5 minutes. From the cooling curve as at 30 minutes (Figure 17), it will be observed that the mould is not as heated up as in sand casting due to the high thermal conductivity of iron. In fact, the mould temperature does not exceed 100°C. There is uniformity in the cooling pattern of the mould, as a result of the good thermal conductivity of cast iron. From Figure 18**,** an interesting result crops up. From the trend of cooling, it will be expected that casting will cool faster than if it were a sand mould. But this assumption is dispelled, considering that the casting cools in about 3 hours compared to about 2 hours of the sand casting. The reason for this is attributed to the high specific heat capacity of cast iron, 210 J/kgK, compared to that of sand, 0.19 J/kgK. Hence cast iron retains heat more than sand, resulting in a longer cooling time. It will also be noted that the cast and the mould cool in approximately the same time as opposed to sand casting.

6. 0 Conclusion

In this work, we have explored the use of the finite element method in the study of the cooling process in castings. The cooling rate was observed from cooling curves generated from the temperature history of the castings. The cooling times obtained from these simulations were compared with the values obtained from experiments and the values compare well. The strains and stresses developed during cooling were also generated from the thermal history using a one way coupling technique. All these were studied for various cooling media like water, air, sand mould and cast iron mould.

References

[1] Kalpakjian, S. (1992), Manufacturing Engineering and Technology, 2nd Edition. Addison-Wesley Publishing Company Inc., New York.

[2] Reddy, J.N. (1993), An Introduction to the Finite Element Method. McGraw-Hill, New York,

[3] Burnett, D.S. (1987), Finite Element Analysis: From Concepts to Application. Addison-Wesley Publishing Company Inc., New York.

[4] Eastop, T.D. and McConkey, A.(1993), Applied Thermodynamics for Engineering Technologists. Longman Group, UK Ltd.

[5] Francis, J.D.(2002), Welding Simulations of Aluminium Alloy Joints by Finite Element Analysis. MSc Thesis, Faculty of the Virginia Polytechnic Institute and State University, Blacksburg, Virginia.